Analytica Chimica Acta 1092 (2019) 9–16

Contents lists available at ScienceDirect

Analytica Chimica Acta

journal homepage: www.elsevier.com/locate/aca

Vacuum-assisted headspace single-drop microextraction: Eliminating interfacial gas-phase limitations

Elefteria Psillakis [a, *], Niki Koutela [a], Agustín J. Colussi [b]

[a] Laboratory of Aquatic Chemistry, School of Environmental Engineering, Polytechnioupolis, Technical University of Crete, GR-73100, Chania, Crete, Greece
[b] Linde Center for Global Environmental Science, California Institute of Technology, Pasadena, CA, 91125, USA

HIGHLIGHTS

- Gas-phase limitations during HS-SDME sampling exist.
- HS-SDME sampling under vacuum removes interfacial gas constraints.
- Vacuum can improve extraction rates even when analyte uptake by the drop is slow.
- Vacuum removes 96% of gas phase constraints at the gas-drop interface for organic analytes.
- Extraction accelerations are discussed as functions of K_H and H_{OA}.

GRAPHICAL ABSTRACT

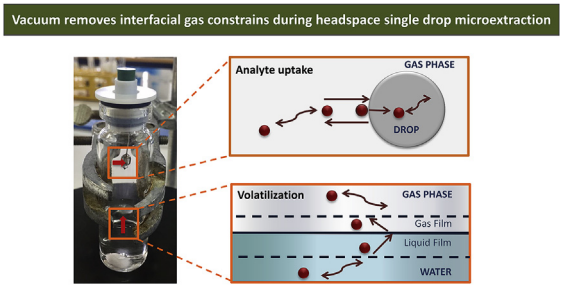

ARTICLE INFO

Article history:
Received 3 July 2019
Received in revised form
18 September 2019
Accepted 21 September 2019
Available online 24 September 2019

Keywords:
Vacuum-assisted headspace single drop microextraction
Headspace single drop microextraction
Gas constraints
Reduced pressure
Analyte evaporation
Analyte uptake

ABSTRACT

Gas-phase limitations have been neglected in headspace single-drop microextraction (HS-SDME) and rate control has been assumed to primarily reside in the liquid water and/or organic phases, but not in the headspace. Herein we demonstrate the presence of interfacial gas constraints and propose using reduced headspace pressures to remove them. To describe the pressure dependence of HS-SDME, the system was decoupled into two interfacial steps: (i) the evaporation step (water-headspace interface) formulated using the two-film theory and (ii) the analyte uptake by the microdrop (headspace-microdrop interface) formulated using the resistance model. Naphthalene, acenaphthene, and pyrene were chosen as model analytes for their large Henry's law solubility constants in n-octanol ($H_{OA} > 10^3$ M atm^{-1}), and their low to moderate Henry's law volatility constants in water as a solvent (K_H). We have found that extraction times were significantly shortened for all analytes by sampling at pressures well below the 1 atm used in the standard HS-SDME procedure. The acceleration of naphthalene extraction, whose facile evaporation into the headspace had been assumed to be practically pressure independent, highlighted the role of mass transfer through the interfacial gas layer on the organic solvent drop. The larger accelerations observed for acenaphthene and (especially) pyrene upon reducing the sampling pressure, suggested that gas-sided constraints were important during both the evaporation and uptake steps. Model calculations incorporating mass transfers at the headspace-microdrop interface confirmed that gas-phase resistance is largely eliminated (>96%) when reducing the sampling pressure from 1 to 0.04 atm, an effect that is nearly independent of analyte molecular mass. The relative importance of the two interfacial steps and their gas- and liquid-phase limitations are discussed, next to the use of K_H and H_{OA} to predict the positive effect of vacuum on HS-SDME.

* Corresponding author.
E-mail address: elia@enveng.tuc.gr (E. Psillakis).

https://doi.org/10.1016/j.aca.2019.09.056
0003-2670/

1. Introduction

Solvent microextraction has gained wide acceptance in the past two decades for being simple, fast and low cost [1–3]. Among the different methodologies that evolved from this approach, single-drop microextraction (SDME) used a microdrop of a water-immiscible organic solvent exposed directly to an aqueous sample [4]. The procedure was very similar to that of solid-phase microextraction (SPME), except that microvolumes of a liquid solvent were used as extracting phase instead of a coated SPME fiber [3,5]. In an attempt to improve microdrop stability and prevent drop contamination from the sample, the headspace SDME (HS-SDME) sampling mode was introduced, where the hanging microliter drop was exposed to the headspace above the sample [6–8].

Previous studies have analyzed the parameters affecting mass transfer rates in HS-SDME. Theis et al. were the first to propose that the transport of relatively volatile analytes such as benzene, toluene, ethylbenzene, and xylene (BTEX) from aqueous samples to the microdrop was limited by slow molecular diffusion rates in the liquid phases [6]. In 2007, Fiamegos and Stalikas presented a theoretical analysis of in-drop derivatization HS-SDME of formaldehyde and hexanal as model compounds [9]. This analysis assumed fast equilibration between water and the headspace as a result of the analytes' low vapor pressures and concluded that overall transfer rates were largely determined by diffusive-reactive processes within the microdrop [9]. In 2008, Schnobrich and Jeannot [10] reported a steady-state kinetic model study, which accounted for their experimental data on BTEX. These authors also considered that transfer rates for less volatile analytes were exclusively controlled by diffusion in the collecting microdrop, *i.e.*, they assumed fast water-air equilibration for this type of compounds [10].

Although the two systems used to analyze mass transfer in HS-SDME were substantially different (non-reactive *vs.* reactive uptake by the microdrop), both studies assumed that water-air equilibrium is rapidly achieved for low volatility compounds [9,10]. However, according to the guidelines provided by Mackay and Yuen [11], the volatilization of organic solutes with a small Henry's law constant (K_H) value (such as formaldehyde) is slow or even unimportant. Moreover, this interpretation neglected the multi-stage process that should take place during HS-SDME sampling of analytes having a small K_H value and a large organic solvent-headspace partition constant. Similarly to headspace SPME sampling (HS-SPME) [12,13], these analytes have a low headspace capacity (small K_H) and cannot be exclusively extracted from the headspace. During the initial stage of HS-SDME, the microdrop absorbs analyte gas molecules rapidly and analyte uptake is linear with time. As soon as the headspace concentration of the analyte falls below the equilibrium level with respect to the aqueous phase, analyte molecules have to be replenished by the analyte transferred from the liquid sample to the headspace. This causes extraction to be slow as there can only be so many analyte molecules in the headspace, depending on the K_H.

Gas-phase limitations have been implicitly neglected in HS-SDME, by assuming that extraction rates were limited by transport in the bulk liquid phases rather than in the headspace [6,9,10]. The argument for neglecting gas-phase limitations was that mass transfer in the headspace must be a fast process given that diffusion coefficients in the gas-phase (at 1 atm) are typically four orders of magnitude larger than in the liquid phase [3,6,9,10]. This perspective, however, overlooks the significant resistances for mass transfer through gas-liquid interfaces. In this connection, the evaporation rates of low K_H analytes from water were found to be controlled by concentration gradients in the vapor rather than in the condensed phase *i.e.*, gas-phase resistance dominated evaporation rates [14,15]. Moreover, in a recent report by Trujillo-Rodríguez et al. [16], faster HS-SDME extraction rates were observed upon lowering the sampling pressure. In their work, the authors reported shorter equilibration times (*vs.* atmospheric pressure extractions) with the so-called vacuum-assisted HS-SDME (Vac–HS–SDME) for several short-chain free fatty acids having a low affinity for the headspace [16]. The experimental results obtained in that study pointed to the importance of interfacial gas-phase constraints in HS-SDME.

The present report addresses for the first time interfacial gas-phase limitations occurring during HS-SDME, by providing evidence that they affect both the evaporation and uptake steps. Vac–HS–SDME is used as the study approach and three polycyclic aromatic hydrocarbons are used as model compounds. A numerical model that quantifies the pressure dependence of extraction rates is presented, and the theory is related to the experimental data. The overall goal is to demonstrate the significance of interfacial gas-phase constraints in HS-SDME, and how they can be removed by lowering the sampling pressure.

2. Theoretical model

2.1. Pressure independence of Vac–HS–SDME at equilibrium

To provide a framework for interpreting our experimental results (see below) we present our theoretical analysis of HS-SDME. In HS-SDME, analytes transfer through the three bulk phases involved (water, headspace, and solvent) and two interfaces (water-headspace and headspace-solvent) until equilibrium is reached. The amount of analyte extracted at equilibrium is independent of the total pressure because partition coefficients and equilibrium concentrations are affected only at high pressures [17].

2.2. Pressure dependence of Vac–HS–SDME under non-equilibrium conditions

During the dynamic stage of HS-SDME sampling, the rate-limiting steps can be the evaporation of the analyte to the headspace, the uptake by the solvent drop, or both, depending on the experimental conditions, and the physical properties of the sample matrix, analytes and extracting solvent. To describe the pressure dependence of Vac–HS–SDME under non-equilibrium conditions, the HS-SDME system is decoupled into water-headspace (evaporation step) and headspace-microdrop (analyte uptake by the microdrop) mass transfers. The model explicitly incorporates the pressure dependence of the rates of each interfacial step. Below, we use two variants of "Henry's Law constants" [18]. The "Henry's law volatility constant", K_H (in atm m^3 mol^{-1}) applies to the water-headspace equilibrium and equals to the ratio of the partial pressure of analyte in the gas phase over the analyte concentration in the aqueous phase. For the headspace-microdrop equilibrium, we use the "Henry's law solubility constant" H_{OA} (in M atm^{-1}), which is the ratio of the analyte concentration in the microdrop phase (*n*-octanol in this study) over the partial pressure of the analyte in the headspace.

2.2.1. Pressure dependence of the evaporation step (water-headspace system)

The pressure dependence of the organic solute evaporating from water is based on the two-film concept, which assumes the existence of analyte concentration gradients in the thin gas- and liquid-films adjacent to the interface, and well-mixed bulk water and air phases [15,19]. Analytes transfer by molecular diffusion through these films and, depending on the properties of the solute, the

resistance to evaporation may arise from transfer through the liquid-film, the gas-film, or both. Past studies reported that for $K_H \leq 1.6 \times 10^{-4}$ atm m^3 mol^{-1} gas-phase resistance represents more than 50% of the overall resistance to evaporation [15]. For these analytes, the equilibrium between the water and headspace will be established faster when sampling under vacuum conditions, given that gas-phase resistance will be reduced due to the inherent increase in gas-phase diffusion coefficients. Note that lowering the total pressure is not expected to affect the volatilization rates of analytes with $K_H \geq 1.6 \times 10^{-4}$ atm m^3 mol^{-1} because liquid-phase resistance (which is pressure independent) starts to control more than 50% of the evaporation rate [15]. Based on the above, reducing the total pressure is expected to accelerate the evaporation rates of low K_H analytes, so that the sample will respond faster to the concentration drops of the analyte in the headspace during the multi-stage process of non-equilibrium HS-SDME sampling [20]. However, the impact of this acceleration on the overall Vac–HS–SDME extraction rate will also depend on the rate-limiting features of the analyte uptake by the microdrop.

2.2.2. *Pressure dependence of the analyte uptake step (headspace-microdrop system)*

The simplicity of the two-film theory is useful for describing mass transport from the headspace to the solvent drop, especially because of the direct dependence of mass transfer coefficients on diffusion coefficients. The uptake of gas-phase species by liquid surfaces, however, is a complex phenomenon governed by various gas- and liquid-phase parameters and processes [21]. The importance of these couplings was identified in the nonreactive uptake of gas-phase pollutants by atmospheric water droplets having diameters ranging from few micrometers (fog) to thousands of micrometers (rain) [22], liquid organic droplets [23], or even organic coated aqueous droplets [24]. Fig. 1(i) shows a schematic of the various processes that may influence non-reactive gas uptake by a liquid drop: (1) diffusion from the gas-phase to the gas-liquid interface, (2) adsorption and mass accommodation at the interface, (3) dissolution (absorption) and diffusion into the bulk liquid phase, and (4) evaporation from the interface [21]. Different models have been used to interpret laboratory experiments on gas uptake by droplets [25]. In one model, gas-uptake is formulated in terms of resistances, by analogy with electric circuits, defined as the inverse

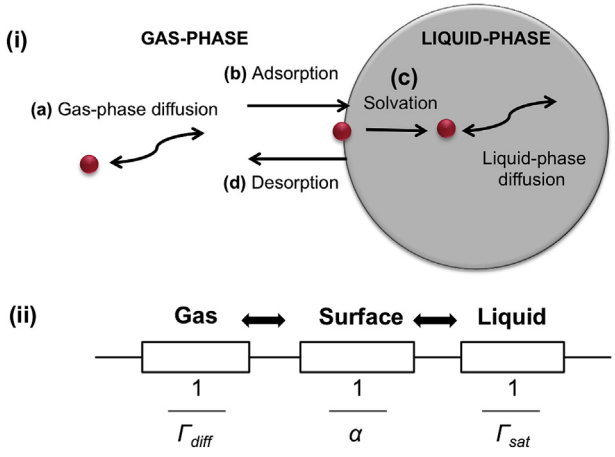

Fig. 1. Schematic representations of (i) the processes that may influence non-reactive gas uptake by a liquid drop: (a) diffusion from the gas-phase to the gas-liquid interface, (b) adsorption and mass accommodation at the interface, (c) dissolution (absorption) and diffusion into the bulk liquid phase, and (d) evaporation from the interface, and (ii) the electrical resistance analogy for gas-phase diffusion, mass accommodation, and solubility limited uptake. Modified from Ref. [21].

of uptake coefficients [21,25]. In this formalism, the resistance of the overall process is obtained by combining the resistances of individual processes in series or parallel (Fig. 1(ii)) [21]. The resistor approach can be used to describe analyte uptake in the headspace-microdrop system during HS-SDME. It can be extended to reactive gas uptake, such as HS-SDME sampling driven by derivatization reactions at the surface of the liquid drop or (after diffusion) in the bulk liquid [21].

The interaction of gases with liquids is described by a net uptake coefficient, γ, in which the mass-transfer rate of molecules to the liquid extracting phase is normalized to the gas kinetic collision rate with the surface [21], and represents the probability that the gas-phase molecule will be taken up by the condensed phase. In the case of non-reactive uptake, the process can be limited by gas-phase diffusion and solubility constraints and the overall uptake process is expressed in terms of a resistance formulation as

$$\frac{1}{\gamma} = \frac{1}{\Gamma_{diff}} + \frac{1}{\gamma_o} \tag{1}$$

where the gas transport coefficient, Γ_{diff}, describes gas-phase diffusion limitation and γ_o is the uptake coefficient in the limit of "zero pressure", *i.e.*, in the absence of gas-phase diffusion limitation [23]. Note that the symbol Γ is used for rates (normalized to collision rates) and can be larger than 1, while the symbol γ is used for probabilities and is always less than or equal to 1 [21]. Among the different methods developed to calculate Γ_{diff}, the Fuchs–Sutugin equation takes into account the effect of gas-phase diffusion on the uptake onto a spherical particle as [21,23,26]

$$\frac{1}{\Gamma_{diff}} = \frac{0.75 + 0.283K_n}{K_n(1 + K_n)} \tag{2}$$

where K_n is the dimensionless Knudsen number defined as $K_n = \lambda/r$, with r denoting the radius of the droplet and λ the gas-phase molecular mean free path. The latter is given by

$$\lambda = \frac{3D_g}{\bar{c}} \tag{3}$$

with $\bar{c}$ denoting the average molecular speed expressed as a function of the gas constant, temperature, and the molar mass of the analyte [26], and D_g the gas-phase diffusion coefficient of the trace species. D_g is often given by the Fuller-Schettler-Giddings correlation as a function of the total pressure, P, the molecular weights of air and the analyte (M_{air} and M_A respectively) and the molar volumes of air and the analyte (V_{air} and V_A respectively) [17]

$$D_g = \frac{0.001 \times T^{1.75}\sqrt{\frac{1}{M_{air}} + \frac{1}{M_A}}}{P[(\sum V_{air})^{1/3} + (\sum V_A)^{1/3}]^2} \tag{4}$$

In the absence of surface or bulk reactions, uptake into the bulk of liquid particles proceeds until the solubility equilibrium is reached [27]. The parameter γ_o, seen in Eq. (1), counts for the effects on the gas uptake of the mass accommodation coefficient, α, and liquid-phase diffusion limitations described by the liquid transport coefficient, Γ_{sat}. In a simple approximation γ_o can be decoupled as [28]

$$\frac{1}{\gamma_o} = \frac{1}{\alpha} + \frac{1}{\Gamma_{sat}} \tag{5}$$

A phenomenological description of the entry of gases into liquids is straightforward in terms of the mass accommodation coefficient, which is defined as the probability that a molecule striking a

liquid surface enters into the bulk liquid phase. The value of α depends on the intermolecular interactions between the adsorbing molecule and the surface and can be considered as a surface resistance to uptake. A past report concluded that nearly perfect accommodation ($\alpha = 1$) is to be expected for organics [29].

Once the gas molecule enters the liquid, it diffuses away from the surface into the bulk liquid. The capacity of the droplet to absorb gas molecules is limited by the capacity of the liquid to solvate the trace gas molecules (solubility). With time, the species in the liquid approach Henry's law saturation [30] and the liquid and gas phases are equilibrated, *i.e.*, the rate of molecules transferring from the bulk liquid to the surface and desorbing is equal to the rate of molecules accommodating at the surface, yielding a zero net uptake. The resistance due to solubility limitation (liquid-phase saturation) is expressed as

$$\frac{1}{\Gamma_{sat}} = \frac{\bar{c}}{8RTH_{OA}}\sqrt{\frac{\pi t}{D_S}} \quad (6)$$

where t denotes the analyte-solvent drop interaction time expressed in seconds, D_S is the liquid-phase diffusion coefficient for the molecule in the solvent drop, R is the ideal gas constant (atm L mol^{-1} K^{-1}) and H_{OA} is Henry's law solubility constant in the organic solvent (octanol in the present studies; given in M atm^{-1}). The $1/\Gamma_{sat}$ term increases with increasing interaction time, causing the overall net uptake rate to decrease with time. This reflects the increasing rate of evaporation of analyte molecules back into the gas-phase as their concentration in the solvent drop approaches the solubility limit. It is noted that the contribution of the $1/\Gamma_{sat}$ term in the gas uptake process can be neglected when the liquid phase is well mixed [22]. This, however, does not apply in static HS-SDME where the solvent microdrop is internally stagnant [6].

Combining Eqs. (1) and (5) the resistor model for the uptake coefficient becomes

$$\frac{1}{\gamma} = \frac{1}{\Gamma_{diff}} + \frac{1}{\alpha} + \frac{1}{\Gamma_{sat}} \quad (7)$$

In the headspace-drop system of HS-SDME, the terms $1/\Gamma_{sat}$ and $1/\alpha$ are independent of the total pressure. For a given temperature and droplet size and assuming a small effect of the air-related terms present in the diffusivity correlation (Eq. (4)), reducing the total pressure of the system will increase D_g. This implies that the gas-phase molecular mean free path and, consequently, the Knudsen number will increase, yielding a reduced value for the $1/\Gamma_{diff}$ term. Accordingly, lowering the sampling pressure will reduce interfacial gas-phase resistance and potentially improve analyte uptake by the microdrop during Vac–HS–SDME. However, the impact of this improvement will depend on the relative magnitude of the liquid-phase constraints within the microdrop as expressed in the $1/\gamma_o$ term.

3. Materials and methods

3.1. Chemicals

The main physicochemical values of the three model analytes are given in Table 1 [31]. Naphthalene (Nap) and Acenaphthene (Ace) were purchased from Sigma-Aldrich (Steinheim, Germany) and Pyrene (Py) from Fluka Chemie GmbH (Buchs, Switzerland) at a purity of ≥99%. 100 mg L^{-1} acetone stock solutions were used daily for the preparation of the spiked aqueous samples and were stored in the dark at 4 °C when not in use. n-Octanol was obtained from Riedel-de Haën (Seelze, Germany). Acetonitrile was HPLC grade and was purchased from Honeywell. Deionized water was prepared on a Barnstead EASYpure II water purification system supplied by Thermo Scientific (Dubuque, USA).

3.2. Vac–HS–SDME and regular HS-SDME procedures

A crimp-top Mininert® valve (Sigma-Aldrich) was modified and a hanging solid support was incorporated in the design that ensured a large contact area with the solvent, maintained the extraction solvent static and allowed the use of higher solvent volume. A detailed description of the construction of the modified Mininert valve can be found in the supporting information (Fig. SI-1). For Vac–HS–SDME, the air inside the sampling device containing a magnetic polytetrafluoroethylene (PTFE) stir bar (10 mm 5 mm; Sigma-Aldrich) was evacuated using the setup described in the past [32], and a VP 2 Autovac pumping unit (7 mbar = 0.007 atm ultimate vacuum without gas ballast) manufactured by Vacuubrand (Wertheim, Germany). 7 mL of the aqueous sample containing target analytes were then introduced in the device through the septum using a gastight syringe. The sampler was placed on top of a magnetic and heating stir bath plate (Heidolph MR-Standard, Germany) and the sample was allowed to equilibrate with the headspace at 25 °C for 10 min. After equilibration, 20 μL of n-octanol was deposited on the stainless steel hub and exposed to the headspace of the sample for a preset time. During equilibration and sampling, the temperature was kept at 25 °C. Stirring of the sample was applied at all times (500 rpm speed). After extraction, pressure equilibration was achieved by piercing the septum with an open-end disposable syringe needle. The modified Mininert valve was removed and the drop was transferred into a 250 μL polypropylene insert. 40 μL of acetonitrile was then added and the mixture was used for analysis. For regular HS-SDME, the initial step of air evacuation was omitted and samples extracted under regular atmospheric conditions. The septum of the modified Mininert valve was changed daily. All experiments were run in triplicate.

3.3. High-performance liquid chromatography (HPLC) coupled to fluorescence detection

Separation and detection was performed on a HPLC (Shimadzu Corporation, Kyoto, Japan), equipped with two solvent delivery pumps (LC 10AD VP), a fluorescence detector (RF 10A XL), a

Table 1
Main physicochemical properties of the three PAHs model compounds investigated here including Henry's Law volatility constant values with water as solvent (K_H), Henry's Law solubility constant in octanol as solvent (H_{OA}) and octanol-water partition coefficient (K_{ow}). Values were reported at 25 °C and were taken from EPI Suite [31].

Compound	Molecular Weight	Vapor pressure (mm Hg) [a]	K_H (atm m^3 mol^{-1}) [a]	H_{OA} (M atm^{-1}) [a]	Log K_{ow}
Nap	128.17	0.085	4.40 10^{-4}	4.54 10^3	3.30
Ace	154.21	0.0006	1.82 10^{-4}	4.57 10^4	3.92
Py	202.26	4.5 10^{-6}	1.19 10^{-5}	6.38 10^6	4.88

[a] 1 mmHg = 133.32 Pa; 1 atm = 1.01 10^5 Pa; 1 M = 10^{-3} mol m^{-3}.

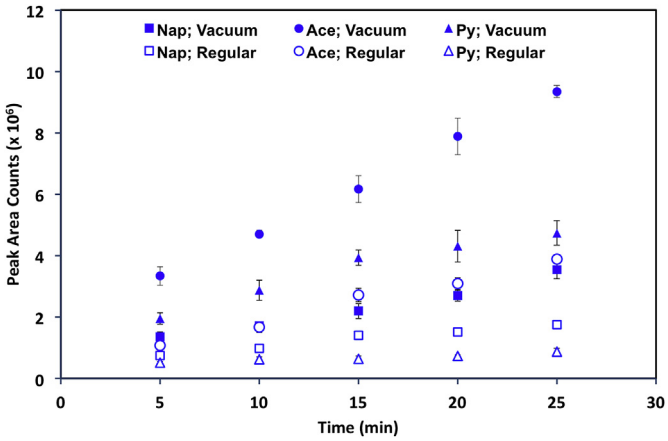

Fig. 2. Extraction time profiles obtained at 25 °C under reduced (Vacuum; filled symbols) and atmospheric (Regular; open symbols) pressure conditions. Other experimental conditions: 20 μL octanol; 7 mL aqueous samples spiked at 10 μg L^{-1}; 500 rpm agitation speed. Some error bars are too small to be visible as compared with the physical size of the symbol.

Rheodyne manual sample injector valve with a 20-μL loop (Chrom Tech Inc., MN, USA) and a Macherey-Nagel C18 (250 mm × 3.0 mm i.d., with 5 μm particles size) purchased from Macherey-Nagel (Germany). The mobile phase consisted of an acetonitrile:water mixture (85:15 v/v) at a 1.0 mL min^{-1} flow rate. The excitation/emission wavelength pairs selected for detection were: 280/355 (Nap and Ace) and 236/398 (Py). A typical HPLC chromatogram can be found in the supporting information (Fig. SI-2).

4. Results and discussion

4.1. Theoretical calculations and relation to analytical results

The effect of sampling time was investigated at 25 °C under low and atmospheric pressure conditions. The sampling times ranged between 5 and 25 min, which is typical for HS-SDME analyses. The results (Fig. 2) showed that at each sampling time tested, Vac–HS–SDME sampling improved the extraction efficiencies of all analytes compared to regular HS-SDME. The positive effect of vacuum on HS-SDME recorded here, experimentally confirmed the theoretical prediction that next to liquid-phase constraints in the water and/or organic drop, interfacial gas-phase limitations may also affect HS-SDME extraction rates, and that lowering the sampling pressure can enhance HS-SDME signals.

Based on the data presented in Fig. 2, at 25 min the resulting Vac–HS–SDME/HS-SDME peak area ratios were sufficiently larger than 1 (2, 3 and 6 for Nap, Ace and Py respectively), suggesting that all analytes were still away from equilibrium. Note that at equilibrium extraction efficiencies are independent of the total pressure and this ratio equals 1. For Nap, the recorded improvement in extraction efficiency at each sampling time was an unexpected result. Nap is an intermediate K_H compound and resistance to evaporation from water was reported to be largely (by 82.2%) liquid-phase controlled [15]. The volatilization rate of Nap was therefore expected to remain relatively insensitive to changes in the total pressure. It should be mentioned here that with HS-SPME (where the mass transfer of semi-volatiles in the headspace-SPME fiber system is a fast process), sampling under reduced pressure conditions was not found to accelerate the extraction of Nap compared to regular pressure conditions [33]. The persistence of the positive effect of vacuum even after sampling the headspace for 25 min, suggested that there was another gas-phase limiting interfacial step in the process, that of Nap uptake by the octanol. This unexpected result was the first experimental evidence that vacuum conditions can improve extraction even when mass transfer from the headspace to the microdrop is a slow step, and implied that as long as interfacial gas-phase diffusion in the water-headspace and/or headspace-microdrop system(s) are/is rate-controlling, reducing the sampling pressure will improve HS-SDME extraction efficiency.

The application of a low sampling pressure also improved the extraction of Ace and especially Py. For the latter, extraction rates at 1 atm were very low and only small changes in extraction efficiency could be recorded when increasing the sampling time. Based on the K_H values of Ace and Py, interfacial gas-phase resistance controlled their evaporation rates by close to 50% for Ace and more than 95% for Py [20]. Lowering the sampling pressure was therefore expected to accelerate mass transfer from water to the gas phase (as seen with HS-SPME under vacuum conditions [33]), so that these analytes could reach the extracting phase through the headspace faster. Nonetheless, the possibility of gas-phase limitations in the headspace-microdrop interfacial system could not be excluded and will be discussed later. At this point and based on the experimental data obtained, the relative importance of the two interfacial systems on the overall extraction rate was not clear.

In the present experimental setup, the extracting solvent could not attain an ideal spherical shape nor have the size of an ideal 20 μL microdrop. Nonetheless, the theoretical calculations and treatment of an ideal 20 μL spherical drop could assist better understanding the effect of pressure on HS-SDME. The gas-diffusion coefficients of all target analytes were calculated at 25 °C using Eq. (4) and the resulting values were used to calculate gas-phase resistances ($1/\Gamma_{diff}$) under regular (1 atm) and vacuum pressure conditions. The ultimate low pressure provided by the pump used here (0.04 atm) was considered as "under vacuum conditions". The resulting values (Table 2), showed that reducing the sampling pressure from 1 to 0.04 atm improved D_g values more than 25 times for each target analyte and resulted in a 96% reduction of the $1/\Gamma_{diff}$ term for each target analyte. This remarkable decrease in gas-phase diffusion resistance captured the effect of lowering the sampling pressure during Vac–HS–SDME. Table 2 also shows that under each pressure condition the $1/\Gamma_{diff}$ values were similar for all target analytes. This pointed out that the impact of reducing the total pressure should be the same for organic molecules with different molecular masses. Concerning gas-particle interactions, several gas-phase organic compounds with molecular masses varying by an order of magnitude were previously found to exhibit similar K_n values at a given pressure [26]. This is because for a given drop size, the average molecular speed, $\bar{c}$, is proportional to the reciprocal of the square root of the molecular mass. At the same time, D_g decreases with increasing molecular mass, as bigger molecules move more slowly and have larger collisional cross sections (Eq. (4)). Hence, for a given temperature, drop size and total pressure, the effect of molecular masses largely cancels out for the mean free paths, λ, and organic analytes will exhibit very similar K_n and $1/\Gamma_{diff}$ values, although their molecular masses may vary considerably. This implies that reducing the pressure from 1 to 0.04 atm should result in a somewhat "fixed" reduction of the $1/\Gamma_{diff}$ term for organics. The magnitude of the liquid-phase constraints should then decide on the effect of low sampling pressure on the headspace-microdrop system. If rate-control is in the liquid-phase of the microdrop, then this "fixed" reduction on interfacial gas-phase constraints might not be sufficient to improve analyte uptake rates. On the contrary, in cases where interfacial gas-phase limitations control analyte uptake (*i.e.* liquid-sided constraints are negligible), then reducing the sampling pressure will accelerate the kinetics of this process.

Table 2
Calculated values for an ideal spherical 20 μL octanol drop (1.684 10^{-3} m radius) at 25 °C, used for estimating $1/\Gamma_{diff}$ under regular and vacuum pressure conditions.

Compound	$\bar{c}$ (m s^{-1})	Regular pressure conditions (1 atm)				Vacuum pressure conditions (0.04 atm)			
		D_g (m^2 s^{-1})	λ (m)	K_n	$1/\Gamma_{diff}$	D_g (m^2 s^{-1})	λ (m)	K_n	$1/\Gamma_{diff}$
Nap	222	6.5 10^{-6}	8.8 10^{-8}	5.2 10^{-5}	14323	1.6 10^{-4}	2.2 10^{-6}	1.3 10^{-3}	565
Ace	202	5.4 10^{-6}	8.0 10^{-8}	4.7 10^{-5}	15818	1.4 10^{-4}	2.1 10^{-6}	1.3 10^{-3}	592
Py	177	5.0 10^{-6}	8.5 10^{-8}	5.1 10^{-5}	14799	1.3 10^{-4}	2.2 10^{-6}	1.3 10^{-3}	576

The calculation of diffusion depths in the octanol drop and subsequent comparison with the final size of the microdrop after covering the hub is unfeasible here. However, Fig. 2 shows that at 25 °C the system is away from equilibrium, suggesting that Eq. (6) describing $1/\Gamma_{sat}$ is applicable [21]. To visualize the time dependency of $1/\Gamma_{sat}$, diffusion coefficients in octanol, D_o, were calculated using the Hayduk-Minhas correlation [23,30], yielding values of 2.0 10^{-10}, 1.7 10^{-10} and 1.5 10^{-10} m^2 s^{-1} for Nap, Ace, and Py respectively. These were then used to calculate the $1/\Gamma_{sat}$ term for sampling times ranging from 5 to 25 min. Fig. 3 shows the plot of $1/\Gamma_{sat}$ *vs.* time and predicts that solubility constraints are relatively more important for Nap compared to Ace and especially Py where the near-zero values indicated no resistance in diffusion in the octanol phase. It is noted that this trend reflected the increasing values in H_{OA} of the model compounds.

Further elaboration of the results consisted of calculating the $1/\gamma_o$ term by taking into account the unity mass accommodation values proposed during the non-reactive uptake of low molecular weight PAHs by neat n-octanol [34]. The $1/\Gamma_{diff}$ and $1/\gamma_o$ terms were summed and the overall resistance to analyte uptake, $1/\gamma$, was calculated as a function of time. Fig. 4 gives the $1/\gamma$ *vs.* time plot (calculations up to 25 min are included) and depicts the dramatic effect of lowering the pressure on Nap, Ace and Py uptake by the microdrop. Fig. 4 also predicts that for all target analytes, interfacial gas-phase limitations dominate analyte uptake by the 20 μL microdrop. These theoretical calculations can be related to the results obtained for Nap, as for this intermediate K_H analyte, volatilization from water to the headspace should be relatively insensitive to changes in the total pressure. Based on these theoretical calculations, rate-control in the gas-phase rather than

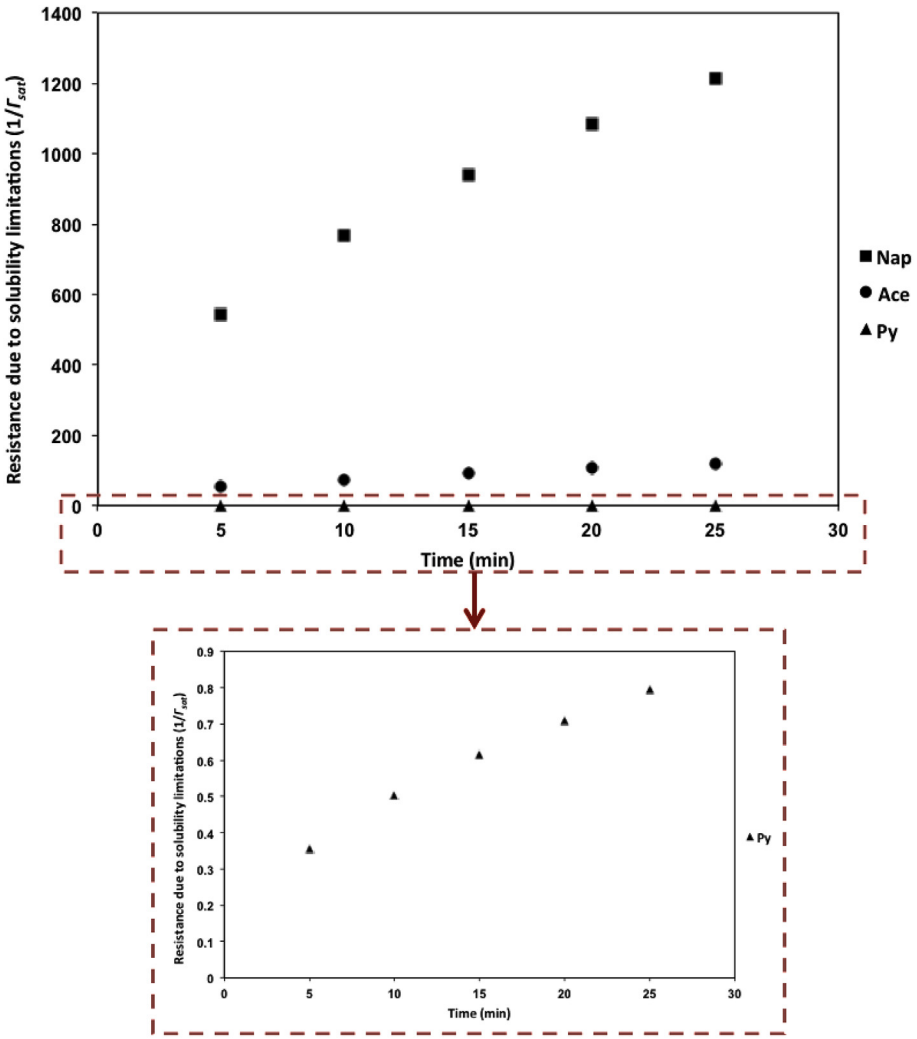

Fig. 3. Calculated time dependency of $1/\Gamma_{sat}$ for each analyte during uptake by an octanol drop at 25 °C.

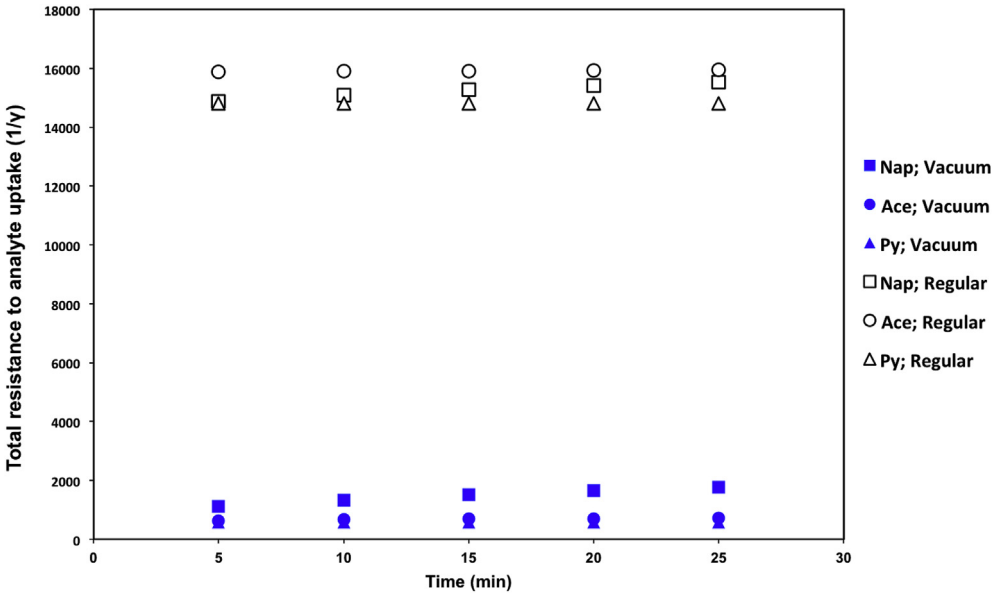

Fig. 4. Time dependency of the total resistance to analyte uptake ($1/\gamma$) by a 20 μL octanol drop at 25 °C, under vacuum (0.04 atm; filled symbols) and regular (1 atm; open symbols) pressure conditions.

in the octanol drop exists for Nap and was experimentally evidenced by the improvement in extraction efficiency when applying the Vac–HS–SDME approach. For Ace and (especially) Py, resistance in the gas-phase controlled the evaporation rates (sample-headspace system) as well as the uptake by the microdrop (headspace-microdrop system). For these two analytes, recorded accelerations when lowering the sampling pressure were related to the removal of gas-sided constraints in the two interfacial systems involved.

4.2. Further implications of the current findings

The current experimental findings suggest that the K_H criterion, previously established to predict the effect of low sampling pressure on HS-SPME, should be used with caution as it describes the requirements to be met in the sample-headspace system and assumes fast equilibration between the headspace and the SPME fiber. However, this may not be the case for HS-SDME. For example, the K_H value of Nap did not meet the K_H criterion, suggesting no effect of vacuum on headspace microextraction sampling. Nonetheless, Vac–HS–SDME sampling was found to be beneficial, as Nap uptake by the solvent drop was a slow step and in particular, interfacial gas-phase diffusion limitations dominated Nap uptake by the octanol microdrop. Based on Eqs. (6) and (7) and assuming $\alpha = 1$ for organics, liquid-phase constraints will not dominate in the headspace-microdrop system for analytes with a $H_{OA} > 10^3$ M atm^{-1} (*e.g.*, model compounds used in the present study) [24]. Accordingly, for analytes with an intermediate K_H value, improvements in HS-SDME will still be recorded when sampling under vacuum conditions, as long as these analytes also have a large H_{OA} value. For low K_H compounds, reducing the total pressure will improve evaporation rates in the sample-headspace system. However, the overall extraction kinetics will be improved only if solubility constraints in the headspace-microdrop system are not controlling the overall extraction rates, *i.e.* analytes with $H_{OA} > 10^3$ M atm^{-1} [24]. For analytes with a $H_{OA} < 10^3$ M atm^{-1}, resistance in the octanol-phase will dominate analyte uptake by the drop and vacuum will improve the overall extraction rates only if evaporation is the limiting step in the overall HS-SDME process and evaporation rates are gas-phase controlled (*i.e.*, low K_H compounds).

The experimental setup used here did not allow studying the effect of microdrop volume. Nonetheless, the theoretical model predicts that the use of smaller microdrop volumes under low-pressure conditions should reduce even further gas-sided limitations [21]. Theoretical calculations at 25 °C using Eq. (4) revealed that the $1/\Gamma_{diff}$ term of the three model compounds will be reduced by more than 98% when moving from regular HS-SDME sampling (1 atm) using a 20 μL octanol drop to Vac–HS–SDME sampling (0.04 atm) using a 1 μL octanol drop. It is noted that the expected enhancement of rate constants with decreasing organic-phase volume has been theoretically predicted in the past [10]. Moreover, in a previous report investigating the effect of drop volume on Vac–HS–SDME, the increase in extraction efficiencies with decreased microdrop volumes were assumed to be due to faster diffusion in smaller drop volumes [16]. However, this assumption is not valid as diffusivity in the liquid phase depends on the physicochemical properties of the analyte and the extracting phase rather than the size of the liquid phase.

5. Conclusions

The present work provides evidence of the relevance of interfacial gas-liquid resistances in HS-SDME extraction kinetics. It demonstrates that vacuum conditions can improve extraction even when mass transfer from the headspace to the microdrop is the slow step in HS-SDME overall kinetics. It also presents a numerical model that rationalizes present findings and predicts experimental outcomes under different scenarios. Model calculations suggest that applying vacuum during HS-SDME sampling leads to a ~96% reduction of the interfacial gas-phase resistance in the headspace-microdrop analyte transfer. They also predict that this reduction is general for most organics. The actual impact of this procedure on overall extraction kinetics will depend on the relative magnitude of the interfacial liquid-phase constraints in water and extracting solvent.

The current experimental findings suggest that the K_H criterion, previously established to predict the effect of low sampling pressure on HS-SPME, should be used with caution and that the value of H_{OA} may provide useful information for predicting the positive effect of vacuum on HS-SDME. Here, octanol was used as the extracting phase and the corresponding H_{OA} values were readily accessible for most organic compounds of environmental importance. However, when another organic solvent is used, partition coefficients might not be available in the literature. In these cases, it is suggested to investigate experimentally the effect of vacuum on HS-SDME sampling.

Declaration of competing interest

The authors declare that they have no known competing financial interests or personal relationships that could have appeared to influence the work reported in this paper.

Appendix A. Supplementary data

Supplementary data to this article can be found online at https://doi.org/10.1016/j.aca.2019.09.056.

References

[1] H. Liu, P.K. Dasgupta, Analytical chemistry in a drop. Solvent extraction in a microdrop, Anal. Chem. 68 (1996) 1817–1821, https://doi.org/10.1021/ac960145h.

[2] M.A. Jeannot, F.F. Cantwell, Solvent microextraction into a single drop, Anal. Chem. 68 (1996) 2236–2240, https://doi.org/10.1021/ac960042z.

[3] M.A. Jeannot, A. Przyjazny, J.M. Kokosa, Single drop microextraction-Development, applications and future trends, J. Chromatogr., A 1217 (2010) 2326–2336, https://doi.org/10.1016/j.chroma.2009.10.089.

[4] M.A. Jeannot, F.F. Cantwell, Mass transfer characteristics of solvent extraction into a single drop at the tip of a syringe needle, Anal. Chem. 69 (1997) 235–239, https://doi.org/10.1021/ac960814r.

[5] E. Psillakis, N. Kalogerakis, Developments in single-drop microextraction, TrAC Trends Anal. Chem. 21 (2002) 54–64, https://doi.org/10.1016/S0165-9936(01)00126-1.

[6] A.L. Theis, A.J. Waldack, S.M. Hansen, M.A. Jeannot, Headspace solvent microextraction, Anal. Chem. 73 (2001) 5651–5654, https://doi.org/10.1021/ac015569c.

[7] A. Tankeviciute, R. Kazlauskas, V. Vickackaite, Headspace extraction of alcohols into a single drop, Analyst 126 (2001) 1674–1677, https://doi.org/10.1039/b103493f.

[8] A. Przyjazny, J.M. Kokosa, Analytical characteristics of the determination of benzene, toluene, ethylbenzene and xylenes in water by headspace solvent microextraction, J. Chromatogr., A 977 (2002) 143–153, https://doi.org/10.1016/S0021-9673(02)01422-X.

[9] Y.C. Fiamegos, C.D. Stalikas, Theoretical analysis and experimental evaluation of headspace in-drop derivatisation single-drop microextraction using aldehydes as model analytes, Anal. Chim. Acta 599 (2007) 76–83, https://doi.org/10.1016/j.aca.2007.07.068.

[10] C.R. Schnobrich, M.A. Jeannot, Steady-state kinetic model for headspace solvent microextraction, J. Chromatogr., A 1215 (2008) 30–36, https://doi.org/10.1016/j.chroma.2008.11.011.

[11] D. Mackay, T.K. Yuen, Volatilization rates of organic contaminants from rivers, Water Qual. Res. J. 15 (1980), https://doi.org/10.2166/wqrj.1980.006, 83–201.

[12] T. Górecki, J. Pawliszyn, Effect of sample volume on quantitative analysis by solid-phase microextractionPart 1. Theoretical considerations, Analyst 122 (1997) 1079–1086, https://doi.org/10.1039/a701303e.

[13] R. Jiang, E. Carasek, S. Risticevic, E. Cudjoe, J. Warren, J. Pawliszyn, Evaluation of a completely automated cold fiber device using compounds with varying volatility and polarity, Anal. Chim. Acta 742 (2012) 22–29, https://doi.org/10.1016/j.aca.2012.01.010.

[14] C.T. Chiou, V.H. Freed, L.J. Peters, R.L. Kohnert, Evaporation of solutes from water, Environ. Int. 3 (1980) 231–236, https://doi.org/10.1016/0160-4120(80)90123-3.

[15] D. Mackay, P.J. Leinonen, Rate of evaporation of low-solubility contaminants from water bodies to atmosphere, Environ. Sci. Technol. 9 (1975) 1178–1180, https://doi.org/10.1021/es60111a012.

[16] M.J. Trujillo-Rodríguez, V. Pino, J.L. Anderson, Magnetic ionic liquids as extraction solvents in vacuum headspace single-drop microextraction, Talanta 172 (2017) 86–94, https://doi.org/10.1016/j.talanta.2017.05.021.

[17] E. Psillakis, E. Yiantzi, L. Sanchez-Prado, N. Kalogerakis, Vacuum-assisted headspace solid phase microextraction: improved extraction of semivolatiles by non-equilibrium headspace sampling under reduced pressure conditions, Anal. Chim. Acta 742 (2012) 30–36, https://doi.org/10.1016/j.aca.2012.01.019.

[18] R. Sander, Compilation of Henry's law constants (version 4.0) for water as solvent, Atmos. Chem. Phys. 15 (2015), https://doi.org/10.5194/acp-15-4399-2015, 4399–4981.

[19] P.S. Liss, P.G. Slater, Flux of gases across the air-sea interface, Nature 247 (1974) 181–184, https://doi.org/10.1038/247181a0.

[20] E. Psillakis, Vacuum-assisted headspace solid-phase microextraction: a tutorial review, Anal. Chim. Acta 986 (2017) 12–24, https://doi.org/10.1016/j.aca.2017.06.033.

[21] P. Davidovits, C.E. Kolb, L.R. Williams, J.T. Jayne, D.R. Worsnop, Mass accommodation and chemical reactions at gas-liquid interfaces, Chem. Rev. 106 (2006) 1323–1354, https://doi.org/10.1021/cr040366k.

[22] S. Raja, K.T. Valsaraj, Uptake of aromatic hydrocarbon vapors (benzene and phenanthrene) at the air-water interface of micron-size water droplets, J. Air Waste Manag. Assoc. 54 (2004) 1550–1559, https://doi.org/10.1080/10473289.2004.10471013.

[23] H.Z. Zhang, Y.Q. Li, P. Davidovits, L.R. Williams, J.T. Jayne, C.E. Kolb, D.R. Worsnop, Uptake of gas-phase species by 1-octanol. 2. Uptake of hydrogen halides and acetic acid as a function of relative humidity and temperature, J. Phys. Chem. A 107 (2003) 6398–6407, https://doi.org/10.1021/jp034254t.

[24] B.T. Mmereki, S.R. Chaudhuri, D.J. Donaldson, Enhanced uptake of PAHs by organic-coated aqueous surfaces, J. Phys. Chem. A 107 (2003) 2264–2269, https://doi.org/10.1021/jp027361g.

[25] C.E. Kolb, R.A. Cox, J.P.D. Abbatt, M. Ammann, E.J. Davis, D.J. Donaldson, B.C. Garrett, C. George, P.T. Griffiths, D.R. Hanson, M. Kulmala, G. McFiggans, U. Pöschl, I. Riipinen, M.J. Rossi, Y. Rudich, P.E. Wagner, P.M. Winkler, D.R. Worsnop, C.D. O'Dowd, An overview of current issues in the uptake of atmospheric trace gases by aerosols and clouds, Atmos. Chem. Phys. 10 (2010) 10561–10605, https://doi.org/10.5194/acp-10-10561-2010.

[26] M.J. Tang, M. Shiraiwa, U. Pöschl, R.A. Cox, M. Kalberer, Compilation and evaluation of gas phase diffusion coefficients of reactive trace gases in the atmosphere: volume 2. Diffusivities of organic compounds, pressure-normalised mean free paths, and average Knudsen numbers for gas uptake calculations, Atmos. Chem. Phys. 15 (2015) 5585–5598, https://doi.org/10.5194/acp-15-5585-2015.

[27] M. Ammann, R.A. Cox, J.N. Crowley, M.E. Jenkin, A. Mellouki, M.J. Rossi, J. Troe, T.J. Wallington, Evaluated kinetic and photochemical data for atmospheric chemistry: volume VI - heterogeneous reactions with liquid substrates, Atmos. Chem. Phys. 13 (2013) 8045–8228, https://doi.org/10.5194/acp-13-8045-2013.

[28] D.R. Worsnop, Q. Shi, J.T. Jayne, C.E. Kolb, E. Swartz, P. Davidovits, Gas-phase diffusion in droplet train measurements of uptake coefficients, J. Aerosol Sci. 32 (2001) 877–891, https://doi.org/10.1016/S0021-8502(00)00113-0.

[29] J. Julin, P.M. Winkler, N.M. Donahue, P.E. Wagner, I. Riipinen, Surface and bulk accommodation of organic molecules of varying structure, Environ. Sci. Technol. 48 (2014) 12083–12089, https://doi.org/10.1021/es501816h.

[30] H.Z. Zhang, Y.Q. Li, J.R. Xia, P. Davidovits, L.R. Williams, J.T. Jayne, C.E. Kolb, D.R. Worsnop, Uptake of gas-phase species by 1-octanol. 1. Uptake of α-pinene, γ-terpinene, p-cymene, and 2-methyl-2-hexanol as a function of relative humidity and temperature, J. Phys. Chem. A 107 (2003) 6388–6397, https://doi.org/10.1021/jp0342529.

[31] US EPA, Estimation Programs Interface Suite™ for Microsoft® Windows, 4.11, United States Environmental Protection Agency, Washington, DC, USA, 2012.

[32] E. Yiantzi, N. Kalogerakis, E. Psillakis, Design and testing of a new sampler for simplified vacuum-assisted headspace solid-phase microextraction, Anal. Chim. Acta 927 (2016) 46–54. http://doi.org/10.1016/j.aca.2016.05.001.

[33] E. Psillakis, E. Yiantzi, N. Kalogerakis, Downsizing vacuum-assisted headspace solid phase microextraction, J. Chromatogr., A 1300 (2013) 119–126, https://doi.org/10.1016/j.chroma.2013.02.009.

[34] D.J. Donaldson, B.T. Mmereki, S.R. Chaudhuri, S. Handley, M. Oh, Uptake and reaction of atmospheric organic vapours on organic films, Faraday Discuss 130 (2005) 227–239, https://doi.org/10.1039/b418859d.